Synthesis and characterization of ZEin-based Low Density porous Absorbent (ZELDA) for oil spill recovery

Nathan P. Holley, Jin Gyun Lee, Kalliat T. Valsaraj* and Bhuvnesh Bharti*

Cain Department of Chemical Engineering
Louisiana State University, Baton Rouge, LA 70803

*corresponding authors: valsaraj@lsu.edu, bbharti@lsu.edu

Keywords: Pickering emulsion, Emulsion templating, Porous materials, Plant-based nanomaterials, Oil-water separation

Highlights

- Hydrophobic 3D porous oil absorbent is synthesized from a plant-based ecofriendly precursor (corn zein).
- Stable oil-in-water Pickering emulsion is prepared using zein nanoparticles.
- Pore diameter and pore volume of the absorbent are controllable by oil-to-water phase volume ratio.
- Hydrophobization of porous zein material is achieved by flaxseed oil.
- Fabrication of absorbent using iron oxide nanoparticles facilitates a contactless recovery of absorbent after oil-water separation.

Graphical abstract

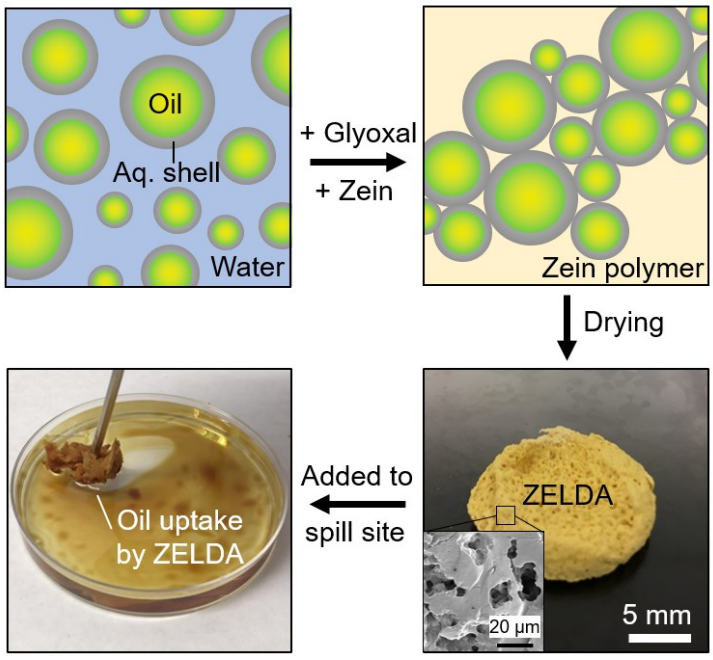

Abstract

Removal of spilled petroleum oil from water bodies using hydrophobic porous absorbent has garnered considerable attention due to the simplicity, large-scale adaptability and robustness of the process. However, the use of nonbiodegradable synthetic oil absorbent during cleanup has raised a secondary concern such as generating plastic pollutants that can accumulate in marine and other ecosystems. To encounter this potential hazard, there is a need to find new biocompatible alternatives to currently used non-degradable porous materials. Here we present ZEin-based Low Density porous Absorbent (ZELDA) synthesized from an emulsion templating method as a new class of naturally derived porous material with tunable hydrophobicity for oil spill recovery. Corn-derived zein nanoparticles are first used to form oil-in-water Pickering emulsion. The addition of polymeric zein into the continuous aqueous phase of the emulsion, and its gradual phase separation enables the formation of a porous matrix. The pore diameter, surface wettability, and oil uptake capacity of ZELDA can be programmed by tuning oil-to-water phase volume ratio of the Pickering emulsion and its selective surface functionalization using flaxseed oil. The synthesis of ZELDA can be further modified with iron oxide nanoparticles to induce magnetic response, which enables its contactless maneuverability and removal from spilled site. The study outlines a new method of synthesis of zein-based porous materials and introduces synthetic routes for controlled surface functionalization, wettability and stimuli responsiveness of the porous material. The synthesized plant-based material provides an ecofriendly alternative to commercially used nonbiodegradable oil sorbents for spilled oil remediation.

1. Introduction

Oil and natural gas exploration, refining, and transportation are possible causes of contamination of the water in the environment [1]. A principal source of on and offshore marine pollution is the spillage of petroleum oil during any of the above processes. Due to the large difference in the surface tension and mass density between water and oil, the spilled oil rapidly spreads out into a thin film on the surface of the water [2]. Several techniques have been introduced to clean up the oil including the use of booms, chemical dispersants, gelling agents, in-situ burning, biodegradation, and absorbents [2–7]. Other methods of oil spill cleanup include skimming, oil herding, bioaugmentation and biostimulation [2,6,8]. However, all these methods suffer from limitations, such as, long cleanup times, potential health hazards to personnel, and negative environmental and ecological impacts. Chemical dispersants are one of the most effective methods to clean up large scale oil spills on the ocean [9]. In the chemical-based oil spill cleanup process, a surfactant solution is added to the spill site which reduces the oil-water interfacial tension and breaks up the spilled oil into small emulsion droplets, thus dispersing i.e. emulsifying the oil in water [10]. However, studies have shown that chemical dispersants and emulsified oil have a significant negative impact on the environment due to some of the potential toxic products generated during their breakdown process [8],[9]. An alternative to such an approach is the complete or partial removal of oil from the spilled site using physical sorbents. Hydrocarbon sorbents can immobilize oil into a solid matrix, containing the oil at spill site and limiting the spreading of oil over a large surface, which would pose significant challenges in a cleanup operation using skimmers and other recovery methods [13].

Oil spill cleanup using physical absorbents is an inexpensive and robust method for the rapid removal of oil from the spilled site [14]. For the oil separation process by absorbents, the spilled oil is preferentially taken up in the pores of an oleophilic absorbent [15]. Currently, polypropylene-based absorbents are widely used for oil spill cleanup due to its hydrophobic nature which enables selective uptake of oil [16]. However, the use of synthetic plastic such as polypropylene as an absorbent incurs the risk of further contaminating the environment by producing microplastics [17]. Microplastics are a class of micron sized particles broken down from plastic waste [18]. Due to their small size, these omnipresent plastic debris can be easily ingested by marine organisms, and their persistence in the food chain has been a great concern on the environment [19]. Therefore, biocompatible oil absorbent can replace the currently used synthetic materials to avoid further contamination of the environment. Such limitations of synthetic polymers can be overcome by adopting a bottom-up synthesis approach and following the principles of *Green Chemistry* [20]. In this article, we demonstrate such a synthetic strategy using zein as a primary precursor for manufacturing a porous absorbent.

Zein is a prolamine (storage) protein found exclusively in the endosperm of the corn kernel. It accounts for ~60 wt.% of the grain and is biocompatible, inexpensive, and widely available as a by-product of the dry or wet milling processing of corn [21–23]. Zein is considered a disposable protein due to its poor water solubility and unbalanced amino acid profile, which makes it difficult for human digestion [23]. Zein has been recognized as a biodegradable scaffolding material used in tissue engineering. Porous zein materials for tissue scaffolding have been synthesized using various methods such as porogen leaching, gas foaming, and freeze drying [24–26]. However, such methods require energy-intensive synthetic processes, and do not provide an immediate control over the stimuli responsiveness (here magnetic), surface chemistry, and wettability of the synthesized porous material. A desired surface wettability and stimuli responsiveness of a porous material is critical for its subsequent application either as tissue scaffold or oil sorbent material. In this article we develop a new approach of synthesizing zein porous material by emulsion templating and provide methods to alter the surface wettability, and magnetic response of the

porous material. Such templating method is facilitated by high solubility of zein an aqueous-alcohol mixture which diminishes upon the gradual evaporation of the alcohol from the mixture (discussed below).

Here we use an emulsion templating method [27] to synthesize the ZEin-based Low Density porous Absorbent (ZELDA). The emulsion templating is a well-established method where the continuous phase undergoes a fluid-to-gel phase transition while preserving the morphology of the dispersed phase. Traditionally, molecular surfactants are used as emulsifiers which function by decreasing the oil-water interfacial tension and prevent the coalescence of the emulsion droplets either by steric or electrical double layer repulsions [28]. However, the surfactants can gradually desorb from the interface due to small adsorption free energy, rendering the emulsion unstable, especially during gelation/polymerization of the continuous phase [29–31]. In contrast, colloidal particles can irreversibly adsorb at the oil-water interface due to its significantly larger adsorption free energy, typically orders of magnitude greater than thermal energy, inducing a higher degree of stability to form the Pickering emulsions [32,33]. The basic properties of Pickering emulsion such as types of emulsion, stability, and size is crucially dependent on the wettability of particles [34,35]. While these properties can be tuned by altering the surface chemistry of synthetic particles, their environmental impact and biocompatibility remains under scrutiny [36–38]. Recently, plant-based colloidal particles have been used as a biocompatible and sustainable alternative to the synthetic particles for biomedical and environmental applications [39–45].

In this article we take advantage of the biocompatibility and higher stability of the oil-in-water Pickering emulsions formed by zein nanoparticles (NPs) to template ZELDA. We use zein NP to stabilize the emulsion and additional zein polymer is introduced in the continuous phase which gradually phase separates and forms the matrix of the ZELDA. We investigate the effect of relative amounts of the two phases on the structural characteristics and porosity of ZELDA. We functionalize ZELDA with flaxseed oil and demonstrate its ability to uptake spilled oil and release it on-demand during a regeneration process. We further demonstrate that the extraction of ZELDA from the water surface can be facilitated by introducing a magnetic response in the material, which we achieve by incorporating iron oxide NPs in the synthesis of ZELDA. The biocompatibility of ZELDA combined with its magnetic responsiveness lays a foundation for the development of an oil sorbent that not only uptakes the spilled oil but responds to external stimuli for easy and safe removal. According a report entitled “Assessment on innovative sorbents” prepared for Bureau of Safety and Environmental Enforcement (BSEE), the median price per gallon of sorbed oil for commercially available sorbents ranged from roughly $2 per gallon to $6 per gallon. We anticipate the large-scale production cost of ZELDA to be similar or more favorable, which would provide a viable eco-friendly alternative to currently used polymeric physical sorbents.

2. Experimental Section

2.1. Materials

Dry α-zein Powder from corn (22-24 kDa, purity ≥ 95%) was purchased from Sigma-Aldrich and was used for zein NP and ZELDA synthesis. The solution of α-zein in 4:1 ethanol-water mixture, where the protein exists in a fully dissolved polymeric state is referred as p-zein. Casein sodium salt (VWR, purity ≥ 95%), and ethanol (VWR, Purity 99.9%) were used as obtained for the synthesis of zein nanoparticles. Anhydrous hexane (Sigma-Aldrich, purity ≥ 95 %), and Triton X-100 were respectively used as oil-phase and non-ionic surfactant of the emulsion. Glyoxal (40 wt-% in H_2O, VWR) was used to crosslink amine groups of the zein in the emulsion. Flaxseed oil for surface hydrophobization of ZELDA was purchased from Sigma-Aldrich which contained 50% α-linolenic acid and it was used without further purification.

2.2. Synthesis of zein NPs

The spherical zein NPs of an average diameter of ~160 nm (Figure S1) were synthesized by a previously established method [46]. In a typical synthesis, 6.0 g of zein was dissolved in 100 mL of 4:1 ethanol-water mixture (by volume) and equilibrated for 1 hour. The resulting mixture was then dispersed in 150 mL of deionized (DI) water containing 3.6 g of sodium caseinate while vigorously stirring. The addition of water leads to supersaturation of zein in the solution, leading to nucleation and growth of zein NPs. This nanoparticle dispersion was then placed in a rotary evaporator at 45 °C for 30 minutes to evaporate ethanol from the mixture. This concentrated mixture is dialyzed in DI water for 24 hours to remove any remaining ethanol from the dispersion. The zein NPs synthesized using this method were stable in aqueous dispersion (zeta potential = -24.3 mV at pH 6.7). Note that the native zein NPs synthesized without sodium caseinate can adsorb at the oil water interface to form Pickering emulsions, however the emulsion stability remains low due to the poor oil wettability of the zein [41]. In our case, the surface modification of the zein NPs with sodium caseinate leads to the formation of an emulsion which is stable for at least 4 months. Such high stability of the emulsion is necessary in the formation of ZELDA by emulsion templating.

2.3. Synthesis of ZELDA

The absorbent ZELDA is synthesized by an emulsion templating method as summarized in Figure 1. The oil-in-water Pickering emulsion is composed of hexane containing nonionic surfactant, Triton X-100, as the discontinuous phase and zein polymer dissolved in 4:1 ethanol-water mixture as the continuous phase. In step 1, 2.0 mL of Triton X-100 (nonionic surfactant) is dissolved in 400 mL hexane. Here hexane is used as a model oil with large vapor pressure, which allows its rapid evaporation and ZELDA formation (see below). In step 2, desired amount of the hexane solution is added to an aqueous dispersion of zein NPs pre-synthesized using the process summarized in section 2.2. This mixture is then sonicated for 30 min and vortexed to form a stable emulsion. In step 3, 0.5 g of glyoxal (crosslinking agent) is added to the 10 mL emulsion to aggregate and interconnect the oil droplets. In step 4, a polymeric zein (p-zein) solution is prepared by dissolving 20 g of zein powder in 100 g of 4:1 ethanol-water mixture. Then, 2.0 mL of this mixture is added to 10 ml of aggregated emulsion prepared in step 3. This mixture of aggregated emulsion and p-zein is dried for 24 hours in a fume hood, followed by complete drying at 60°C in a convection oven to obtain ZELDA. The surface of the ZELDA is further hydrophobized for the oil uptake as summarized in section 3.2.

2.4. Characterization of ZELDA

Sub-samples (1-3mm lateral and 1-2mm thick) were cut from center portions of the solidified ZELDA and prepared for Scanning Electron Microscope (SEM) imaging (Quanta™ 3D DualBeam™ FEG FIB-SEM). The samples were coated with platinum and mounted on a metal sliding using carbon tape. SEM image analysis of product was conducted to characterize the three dimensional (3D) porous structure and morphology variations of ZELDA at different oil-to-water phase-volume ratio (R) used in the templating process (discussed below). In a typical image analysis steps, SEM micrographs were imported in ImageJ software [47] and converted to the 8-bit format. The threshold tool was used to enhance the contrast of the pores and reduce the amount of noise evaluated. The diameter of the pore is determined by the ImageJ's Particle Analyzer plugin. The analysis procedure was performed on at least 5 images at a given R, and frequency distribution of the pore diameter is obtained for ZELDA with R = 5, 7, 10, and 15. The wettability of ZELDA as a function of degree of surface functionalization (using flaxseed oil) was

determined by measuring the contact angle of water on ZELDA pellets. The contact angle measurements were conducted using an Attention Theta optical tensiometer (Biolin Scientific).

3. Results and discussion

3.1. Mechanism of ZELDA formation

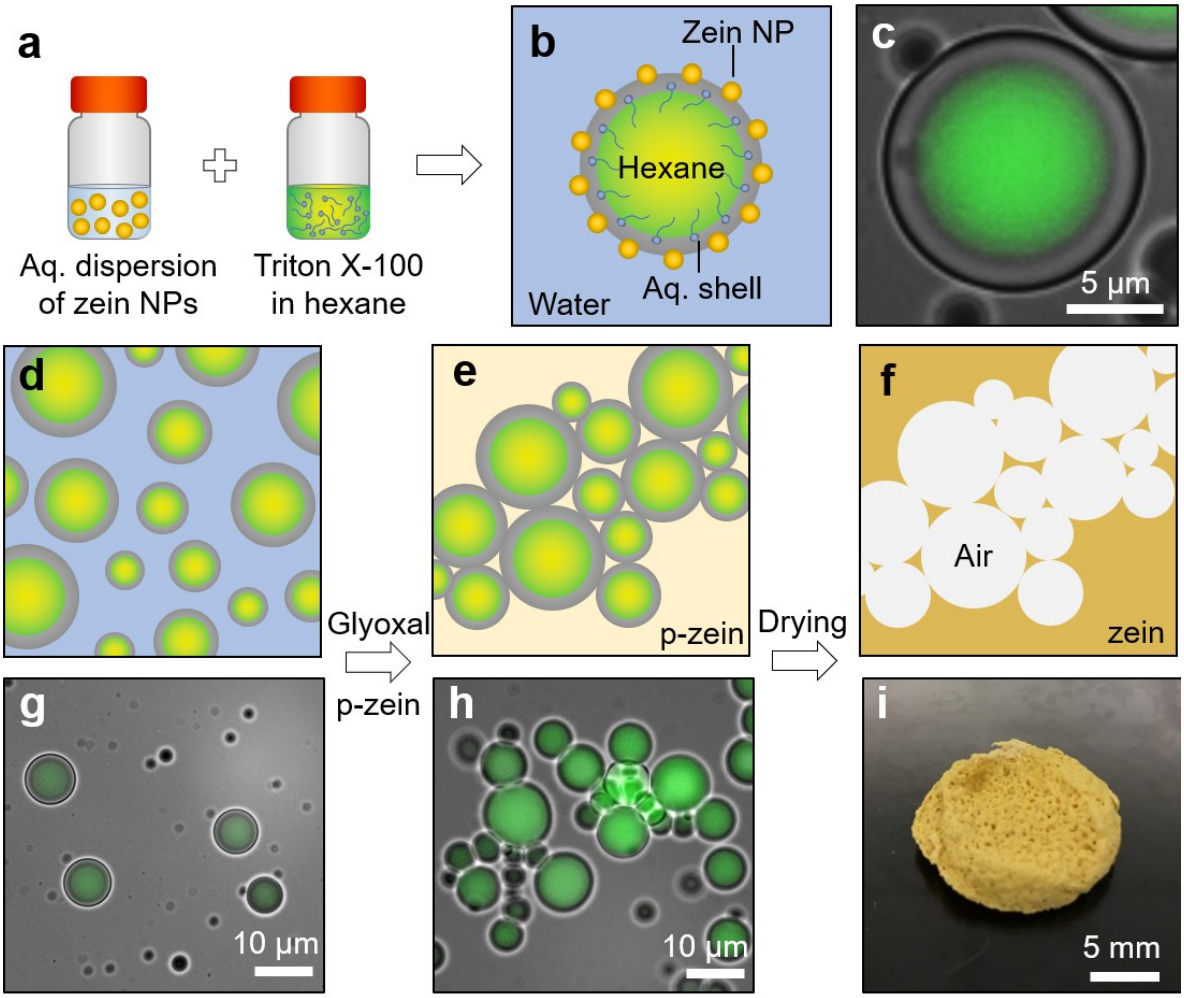

Figure 1. Schematic representation for synthesis of ZELDA (a) Aqueous dispersion of zein NPs and hexane containing non-ionic surfactant (Triton X-100) are mixed to form oil-in-water emulsion. (b-c) Schematic and brightfield-florescent overlaid microscope image of an emulsion droplet showing the structure with an oil core and aqueous layer separated by a layer of zein NPs. The hexane was pre-mixed with Nile Red dye, which appeared green in fluorescent microscope image. (d-f) Schematic, (g-h) microscope images of emulsion initially prepared at R = 7 diluted 20x with DI water for imaging purposes, and (i) photograph showing the transformation of the emulsion into ZELDA. Glyoxal crosslinks zein, which leads to the aggregation of emulsion droplets. (h-i) The addition of the p-zein solution in 4:1 ethanol-water mixture plasticizes the continuous phase and result in a porous matrix formation by gradual precipitation of p-zein. Here p-zein is referred to the solution of zein in ethanol-water mixture where it exists as a completely soluble polymer.

ZELDA is synthesized by templating from an oil-in-water emulsion, where the phase separation of polymeric zein in the continuous medium leads to the formation of the walls of the porous material. The structure and properties of the ZELDA are determined by the relative amounts of oil and water in the templated emulsion. Here we define the phase volume ratio as *R* = volume of oil phase per volume of the aqueous phase. In our experiments, the value of *R* is systematically varied in the range 0-15. The mixture was sonicated and vortexed for 5 minutes to form a stable emulsion. Note that the structure of oil-in-water emulsion droplet is that of a "biliquid foam" viz. polyaphrons, where the oil droplet is encapsulated within the water film [41]. Here we use polyaphrons for the synthesis of ZELDA because of their better stability over traditional emulsions, which is necessary in our case. For the sake of simplicity and to avoid any confusion, we refer to this pickering polyaphron dispersion as the "emulsion" (Figure 1d-i).

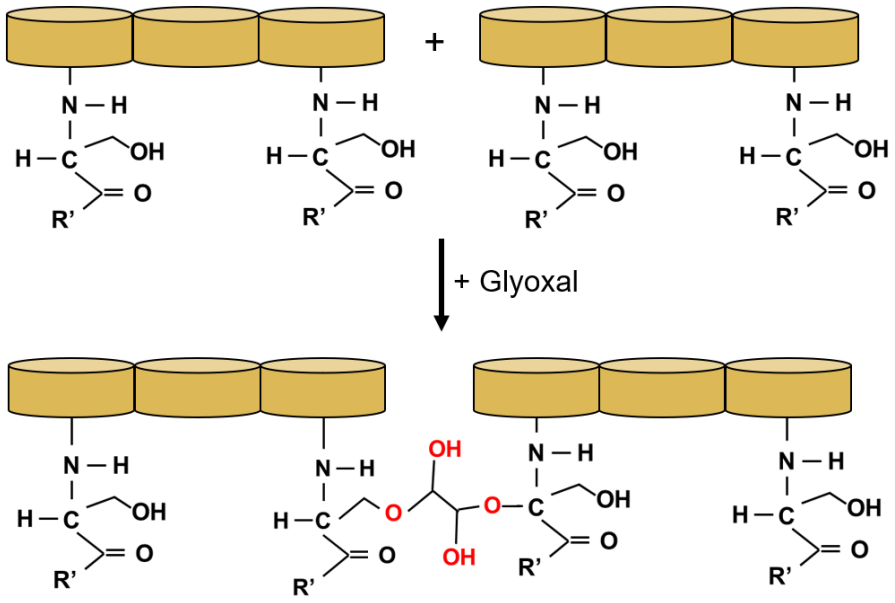

Scheme 1. Schematic representation of the cross-linking of zein protein by Glyoxal, leading to the observed aggregation (interlinking) of the emulsion droplets. Here R' represents the terminal alkyl group of the amino acids forming the zein structure.

The addition of glyoxal cross-links zein NPs surrounding the emulsion droplets by binding to the most exposed glutamine ends of the zein molecules [48]. Zein organizes itself in compact helical structures that are bound to each other through glutamine residues residing at the ends of the helices [49]. This crosslinking forms a bi-layered zein structure, which creates free volume between the stacks of zein [48]. To confirm the role of glyoxal in the synthesis of ZELDA, we investigate the change in the spatial distribution of the emulsion droplets upon the addition of glyoxal (Figure 1g-h, S2). In the absence of glyoxal at *R* = 7, the emulsion droplet diameter is in the range 1–10 μm, and the droplets remain in a dispersed state. The zeta potential of the zein NPs stabilizing the emulsion droplets is -24.3 mV at pH 6.7, which would impart a negative charge to the emulsion droplets leading to their stability in aqueous dispersion due to electrostatic double layer and steric repulsions. Addition of glyoxal leads to the aggregation of the emulsion droplets as shown in (Figure 1h). This aggregation of the droplets is the result of cross-linking of the zein NPs on the surface of neighbouring emulsion droplets, which was not observed in the absence of glyoxal. This method of cross-linking zein is known to enhance the tensile strength of the zein

[50–52], however in our case this crosslinking may further facilitate the formation of interconnected pores in ZELDA.

Finally, ZELDA is synthesized by gradual precipitation of p-zein dispersed in the continuous aqueous phase of the emulsion. Water is a poor solvent for p-zein, but it readily dissolves in a 4:1 ethanol-water mixture. We take advantage of this characteristic of p-zein to first dissolve it in the continuous phase of the Pickering emulsion, then gradually evaporate ethanol, which leads to the precipitation of p-zein in the continuous medium and formation of ZELDA. Note that no porous material formation was observed in the absence of zein NPs, which is likely due to the poor stability of the emulsion template in a 4:1 ethanol-water mixture. Hence, both the presence of NPs, and glyoxal play key roles in the formation of ZELDA.

3.2. Pore structure and hydrophobization of ZELDA

The pore diameter in ZELDA is governed by the oil-to-water phase volume ratio, R of the emulsion used in the templating process. Here we synthesize ZELDA with increasing R from 0 to 15 and visualize its pore structure using a SEM as shown in Figure 2. We find that in the absence of emulsion structure i.e. $R = 0$ Figure 2a, p-zein forms a smooth film, as reported previously [53]. As the value of R is increased, ZELDA shows the presence of spheroidal pores within the continuous matrix of zein as shown in Figure 2b-d. The ZELDA shows the presence of clustered pore structure instead of uniformly distributed and spatially resolved pores. The observed non-spherical pores in ZELDA is due to the aggregation of the template, i.e. emulsion droplets, by glyoxal, as discussed in the previous section and shown in Figure 1h. Further, we obtain pore size distribution by analyzing SEM micrographs using the ImageJ software package [47] (See section 2.2 for details). We find that the average diameter of the pore decreases with increasing R (Figure 2e). Such decrease is attributed to the effective increase in the concentration of Triton X-100 surfactant in the mixture, which is known to govern the size of the emulsion droplets [54]. The increased amount of the surfactant enables stabilizing the larger oil-water interfacial area, thus reducing the size of the emulsion droplets. Note that the decrease in the size of emulsion droplet and corresponding pore size of the templated ZELDA increases the local surface roughness, which can influence the apparent water contact angle of the material [55].

The porous nature of ZELDA leads to a significant decrease in the mass density of the material. We determined the density of ZELDA for $R = 7$ using a model sample. The macroscopic volume of the slice was determined using a Vernier caliper by measuring the length, width, and height of the ZELDA slice. The sample was then weighed, and the density was calculated as mass per volume. We find that the density of ZELDA at $R = 7$ is ~ 0.62 g cm^{-3}, which is higher than typical foams but lower than nonporous polymeric materials, and comparable to that of other low-density adsorbents [56].

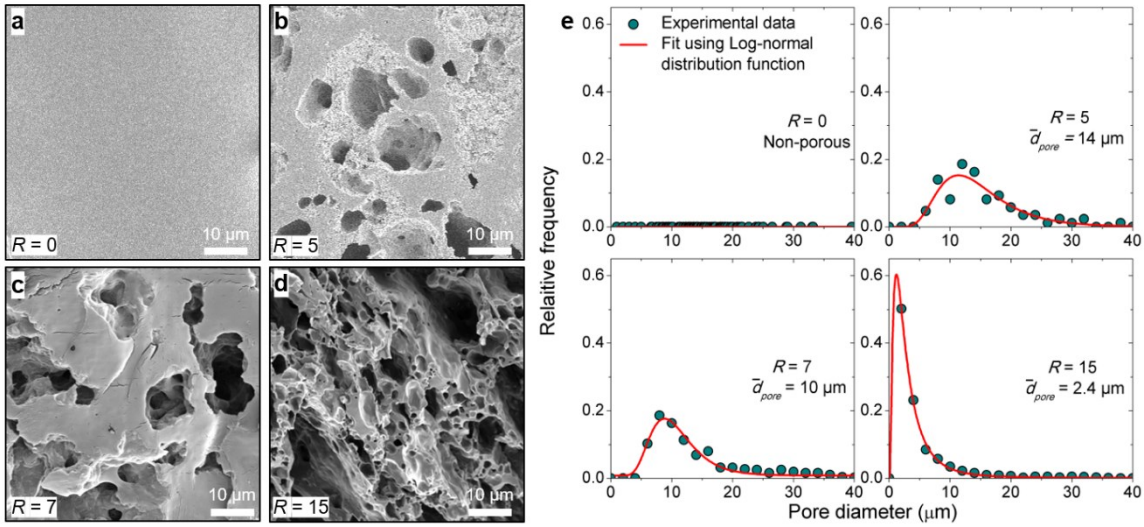

Figure 2. (a-d) SEM images of pores in ZELDA at R = 0 (no visible pore), 5 (a, $\overline{d}_{pore}$ = 14 μm), 7 (b, d_{pore} = 10 μm), 10 (c, $\overline{d}_{pore}$ = 4.6 μm), and 15 (d, $\overline{d}_{pore}$ = 2.4 μm). Here $\overline{d}_{pore}$ is the average pore diameter obtained by fitting the experimental data with a log-normal distribution function shown in (e). (e) Relative frequency of pores as a function of d_{pore} and R. The average pore diameter decreases upon increasing R, but the distribution of pore diameters is narrowed.

A controlled hydrophobization of the zein surface is necessary for selective uptake of oil by ZELDA in oil-water mixture. Unfunctionalized zein protein is hydrophilic and does not allow for a spontaneous surface wetting with oil [57]. To facilitate oil uptake using ZELDA, we functionalize the surface of zein using flaxseed oil, which is of natural origin, biocompatible, and inexpensive [58]. In a typical functionalization experiment, a dried ZELDA structure is saturated with the 20 vol% solution of flaxseed oil in hexane. The saturated ZELDA is then exposed to UV-light for 1 minute to initiate the cross-linking of zein and flaxseed oil then subsequently dried in a convection oven at 50 ºC for 24 hours. During the drying process, α-linolenic acid in the flaxseed oil undergoes the polymerization reaction [59]. In the presence of oxygen, the diene group of linoleic acid undergoes autoxidation [60]. The autoxidation reaction generates a peroxide that is highly susceptible to cross-linking with zein and leads to the formation of a film on the surface of ZELDA. We find that the functionalization of ZELDA does not result in any significant change in pore diameter, indicating that the thickness of hydrophobic layer is significantly smaller than the pore diameter Figure S3.

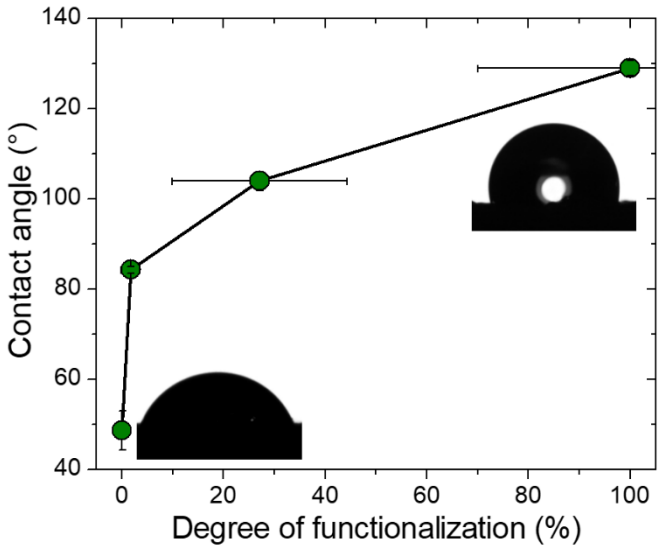

Figure 3. Water contact angle on ZELDA (*R* = 7) at different degrees of flaxseed oil functionalization. As the degree of functionalization is increased, ZELDA demonstrates an increase in hydrophobicity. The inset images show droplet of water on ZELDA with increasing degree of functionalization. The horizontal error bars are the standard deviation of the degree of functionalization estimated for multiple replicates using UV-vis spectrophotometry and a calibration curve (Figure S4). The vertical error bars in the contact angle for most samples were less than the symbol size.

The hydrophobization of ZELDA leads to its preferential wetting with oil. The degree of functionalization of ZELDA was determined by the adsorption isotherm of flaxseed oil on to the surface of ZELDA. In a typical surface functionalization step, ZELDA pellets of known weight were placed in vials with increasing known concentration of flaxseed oil diluted with hexane and left to equilibrate for 24 hours. The absorbance of flaxseed oil in the hexane solvent was determined at λ = 230nm, and a calibration curve was used to determine the initial and final concentration of the flaxseed oil based on the analyte's absorbance intensity Figure S4. The resulting adsorption isotherm depicts a maximum adsorbed amount of 49 mmol g^{-1} which is equivalent to 100% degree of functionalization. To quantify the change in wetting properties of ZELDA, we determine the water contact angle of the material with an increasing degree of surface functionalization. In a typical experiment, a 0.5 µL droplet of DI water is placed on a disc shaped ZELDA pellet, and the contact angle is measured using a high-speed camera. We find that the water contact angle increases from 50° to 130° for ZELDA with *R* = 7, upon its flaxseed treatment highlighting ZELDA changes from water-wet to oil-wet. We further investigate the effect of pore structure on the water contact angle at ZELDA Figure S3a-b. We find that the contact angle is maximum for *R* = 7, which is the result of surface roughness induced transition from Wenzel to Cassie-Baxter wetting regime [61]. Such transitions are well-known for materials with variable surface roughness, as the air pockets between the surface peaks and valleys drive such an increase in the water contact angle [61].

3.3. Oil uptake and release by ZELDA

To understand the relation between the pore structure of ZELDA and its corresponding oil uptake capacity, we systematically measure the oil sorption isotherms. In a typical experiment, a known weight of ZELDA pellet at a given *R* is immersed in 25 mL of Louisiana sweet crude oil for 30 seconds at 25 °C. Then, the saturated ZELDA is removed from the equilibration chamber, and the excessive oil on the surface of ZELDA was removed by drip drying. Drip drying of ZELDA is

conducted by holding the ZELDA sample above the oil bath for one minute allowing for remaining excess oil to be removed from the pellet.

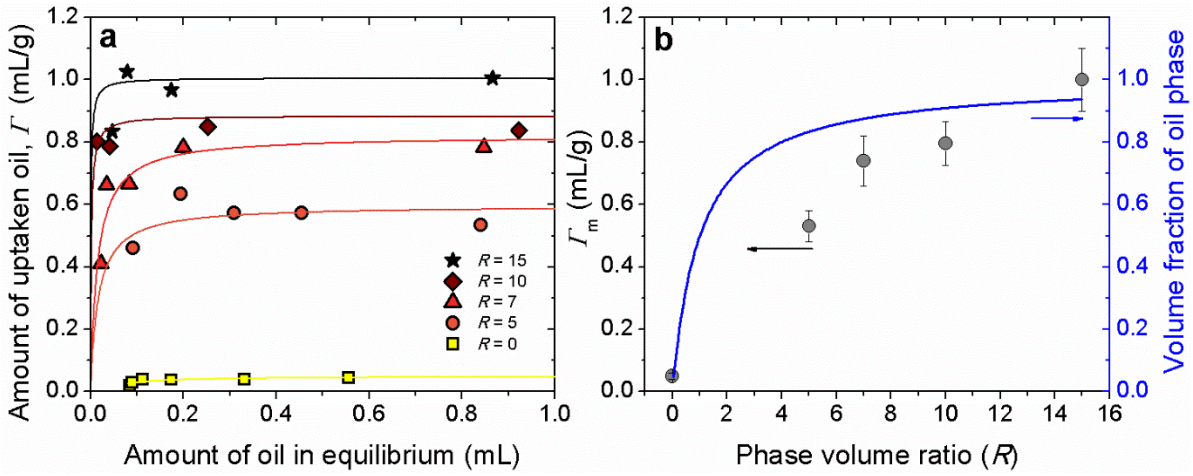

Figure 4. (a) Crude oil uptake isotherm on ZELDA at increasing *R*. The discrete points are the experimental data, and the lines represent the best fit using the Langmuir model given in Equation 1. (b) Maximum oil uptake capacity (Γ_m) (left ordinate) and calculated volume fraction (right ordinate) in the emulsion used for templating ZELDA. The oil uptake capacity of ZELDA increases with increasing *R* due to increase in the net pore volume.

ZELDA with *R* > 0 shows an initial increase in the oil uptake which remains constant as the amount of oil in equilibrium increases. This increase in the adsorbed amount of oil on ZELDA with increasing *R* is attributed to the increase in the pore volume. Here, we use a Langmuir model to find the oil uptake capacity of ZELDA at different *R* and investigate the affinity between oil and ZELDA [62]. The Langmuir model is a two-parameter model widely used for the uptake of oil on the solids. It is expressed as [63,64]

$$\Gamma = \frac{\Gamma_m K c_{eq}}{1+K c_{eq}} \quad (1)$$

where Γ is the amount of crude oil uptake by ZELDA, Γ_m is the maximum oil uptake capacity, K is the equilibrium oil uptake constant related to the affinity between the oil and ZELDA, and c_{eq} is the amount of crude oil in bulk at equilibrium.

We find that only a small amount of oil can be absorbed by the nonporous zein i.e. *R* = 0, highlighting the necessary role of the porous structure of ZELDA in its oil uptake ability. For ZELDA synthesized at *R* > 0, the isotherms show a rapid increase in Γ with increasing equilibrium amount of oil (Figure 4a). This rapid increase in Γ is a signature of strong attraction between the pore-walls of ZELDA and crude oil. The isotherms show an initial increase followed by a plateau on the isotherm, which corresponds to the maximum oil uptake capacity of ZELDA (Γ_m). We find that Γ_m monotonically increases with increasing *R* (Figure 4b). This increase in Γ_m is attributed to an increase in the total pore volume in ZELDA which is dependent on the volume fraction of oil phase in the emulsion used for the templating process (Figure 4b). The oil uptake in ZELDA is driven by the capillary pressure [65]. The capillary pressure, Δp_c is given by the Young-Laplace equation as [66]

$$\Delta p_c = \frac{2\gamma cos\theta}{\overline{d}_{pore}} \quad (2)$$

where γ is the surface tension of the crude oil (γ ~ 22 mN/m), and θ is the contact angle of the oil on ZELDA. As *R* increases, $\overline{d}_{pore}$ shows a linear decrease from 14 μm (*R* = 5) to 2.4 μm (*R* = 15) as shown in Figure 2 and S5, thus an increase in capillary pressure from 3.0 to 32 kPa. An

increase in Γ_m upon decreasing , $\overline{d}_{pore}$ leads to a stronger capillary force in narrow pore due to a wicking effect of oil [67], driving the oil uptake. The maximum oil uptake capacity of ZELDA is probably lower than some of the commercially available polymeric porous materials [14], but further work is necessary to better optimize the internal structure and surface chemistry of ZELDA for maximum oil uptake capacity.

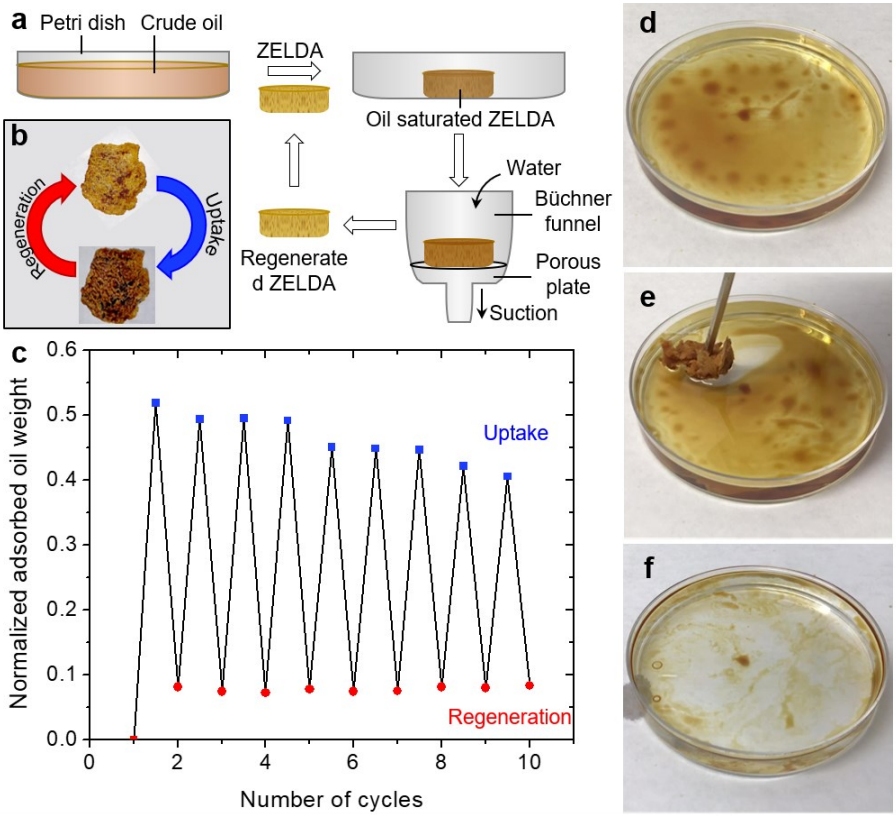

Figure 5. (a-b) Schematic representation of the crude oil uptake and regeneration of ZELDA. The Images in b show dry and oil-saturated ZELDA. (c) Uptake/Regeneration data collected from modified ZELDA (*R* = 7) that underwent ten cycles of the method described showing the cyclic reusability of ZELDA. (d-f) Sequence of photographs showing spilled crude oil cleanup process using ZELDA. The spilled crude oil initially spreads onto water as a thin film, and ZELDA mounted on a metal rod instantly uptakes the spilled oil and leaves the oil-free surface.

ZELDA pellets with *R* = 15 shows the maximum oil uptake capacity owing to its large total volume of pores. However, due to the increased specific pore volume, the mechanical strength of the ZELDA at large *R* is significantly reduced. The material becomes brittle due to the decrease in the pore wall thickness and hence the corresponding mechanical strength deteriorates. Due to such reduction in the mechanical strength at large *R*, we preferred to use *R* = 7 for our subsequent oil uptake and removal experiments.

The oleophilic properties of the ZELDA, as well as their 3D structure with interconnected pores, are promising attributes for selective oil uptake from spilled site (Figure 5). We show the oil/water separation ability of ZELDA in Movie S1 and Figure 5d-f. In a typical experiment, the 1 mL of crude oil was dispersed on the surface of 25 mL water in a petri dish. Then, a ZELDA pellet synthesized at *R* = 7 was added on the surface of the oil, and the change in the state of the oil was monitored using a digital camera. Once ZELDA is added, the oil floating on the surface of

water is readily uptaken in a short time (~1 minute). The porous structure of ZELDA allows for the retention of oil and facilitates its removal from spill site.

The procedure of oil uptake and regeneration of ZELDA is shown in Figure 5a-b. To quantify the oil uptake and regeneration capability of ZELDA, we systematically measure the oil uptake and release for several cycles. In a typical cycle, dry ZELDA is weighed and added to the petri dish containing water and crude oil. The ZELDA is equilibrated for 1 minute and removed from the petri dish using a pair of forceps. The net oil uptake is determined by measuring the difference in the weight of ZELDA in dry and oil-saturated state. The ZELDA saturated with crude oil is then placed in a Büchner funnel atop a vacuum flask. A sink aspirator is attached to the vacuum flask and was used for suction. The ZELDA samples are then rinsed using water for 2 minutes and placed in an oven at 40 °C for 1 hour to dry. The weight of the ZELDA is then remeasured, and the steps of oil uptake and regeneration are repeated for several cycles. The amount of oil uptake and released in ten such cycles is shown in Figure 5c. We find that from the second cycle onwards, the oil uptake capacity of ZELDA begins decreasing gradually with each subsequent cycle Figure 5c. The observed decrease in oil uptake capacity could be attributed to the combination of three factors, namely, retention of oil in ZELDA, partial loss of surface flaxseed coating, and collapse of the internal pore structure. The pore obstruction resulting from either of the above-mentioned processes would prevent further uptake of oil, thus reducing the oil uptake capacity of ZELDA.

3.4. Magnetoresponsive ZELDA and its disposal

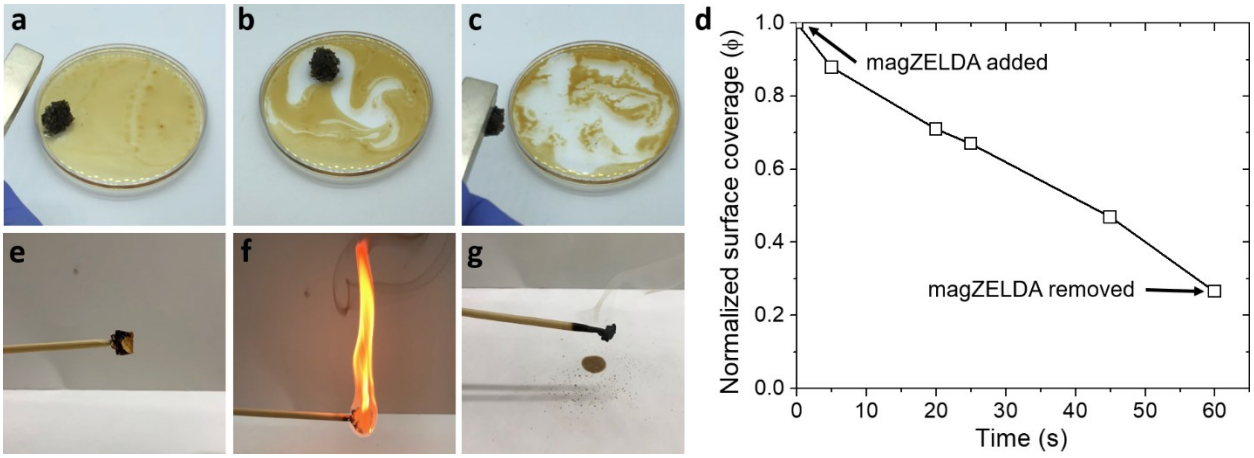

Figure 6. (a-c) Images showing the removal of oil from the surface of water using magZELDA. (d) The change in normalized surface area coverage by oil over time. The observed decrease in the surface area highlights the ability of magZELDA to clean water surfaces contaminated with spilled oil. (e) Oil-saturated ZELDA mounted to a wooden rod, (f) ZELDA ignited from an external flame to determine fuel viability, (g) final ash-like structure remaining after ZELDA is extinguished.

The maneuverability and removal of ZELDA from an affected oil spill area in a contactless manner is highly desirable but, non-trivial to achieve. In order to have such a contactless response, the ZELDA can be modified by including iron oxide (Fe_3O_4) NPs in the synthesis [68]. ZELDA samples with magnetic modification are referred to as magZELDA, which can be directed and maneuvered using magnetic interaction Figure 6a-c, Movie S2. MagZELDA is synthesized in a similar manner as described in Figure 1, however 1 wt-% Fe_3O_4 NPs is added into the p-zein prior to its addition to the emulsion template. The original mass density of ZELDA (0.62 g cm^{-3}) was used to calculate the maximum quantity of Fe_3O_4 NPs (5 g cm^{-3}) that can be incorporated into a sample. It was

determined that magZELDA with a concentration of 8 wt-% Fe_3O_4 NPs would have a density of ~0.97 g cm^{-3} allowing magZELDA to remain buoyant on the surface of water. However, such simple calculation ignores the impact of the magnetic nanoparticles on the pore volume and integrity of structure. The Fe_3O_4 NPs concentration of 1 wt-% in p-zein was used for magZELDA, because it was the lowest concentration of Fe_3O_4 NPs that allowed for the contactless removal of oil laden magZELDA, and did not cause abnormal sample drying during the magZELDA product formation. The magZELDA could uptake crude oil from the surface of the water, and retain it as shown in Figure 6a-c. A rare-earth magnet is used to maneuver the magZELDA to oil-rich surface sites, and removed in a contactless manner as shown in Figure 6c. The oil uptake and removal ability of magZELDA can be quantified by determining the decrease in the surface area occupied by the oil Figure 6d.The zein absorbent can reduce the surface coverage (ϕ) of the oil by ~80%. We performed a long-term stability test of oil-saturated ZELDA, which remained buoyant on the surface of water for over 3 weeks. We believe that magnetic maneuverability of magZELDA will allow for the efficient recovery of the oil laden absorbent, limiting the possibility of uncollected adsorbents in the environment. The ability of ZELDA to selectively uptake oil, magnetically directed and retaining the buoyancy, highlights to potential of the porous materials to be used in oil-spill applications. [69–71].

The high oil adsorption capacity and magnetoresponsive characteristics of ZELDA are essential for the recovery and reuse of oil-laden ZELDA as a fuel source. Since ZELDA itself has value as a fuel, the retrieved oil-saturated adsorbent can be directly burned as a fuel without the need for an oil regeneration step. This is demonstrated by igniting the oil-saturated ZELDA mounted to a wood skewer Figure 6e-g, which leaves behind ash-like material after combustion. During the fuel viability test of ZELDA, it was determined that 1 gram of oil-laden ZELDA synthesized at R = 7 can combust for ~32 seconds after the initial ignition of the sample. The burn time associated with oil-laden ZELDA can be best compared to that of combustion of coal dust, which, depending on the particle size, can have a burn length of 5 – 35 seconds per gram [72]. Here we estimate the calorific value of crude oil laded ZELDA. The energy density of precursors of ZELDA are found in literature, zein (17.01 MJ kg^{-1}) [73], crude oil (42-47 MJ kg^{-1}), hard black coal (> 23.9 MJ kg^{-1}), lignite brown coal (< 17.4 MJ kg^{-1}). Based on these values, we estimate the energy density of approximately 25 MJ/kg for ZELDA with R = 7. This energy density value of ZELDA is comparable to that of coal (17.4 - 23.9 MJ kg^{-1}) and favor its potential use as a fuel. Additionally, the burning of oil-saturated ZELDA as a fuel circumvents the potential risks associated with the waste handling and disposal.

4. Conclusion

We presented a low-density porous absorbent synthesized using zein as a plant-based precursor. The porous material is synthesized by templating zein nanoparticle and Triton X-100 stabilized oil-in-water emulsion. Evaporation of ethanol from the continuous aqueous solvent leads to the phase separation of pre-dissolved polymeric zein and formation of a matrix templating the oil droplets. We show that as oil-to-water phase volume ratio increases, the pore diameter of ZELDA decreases due to an effective increase in the concentration of non-ionic surfactant. The synthesized porous material is further hydrophobized using flaxseed oil for selective uptake of oil by controlled functionalization of ZELDA. The oil uptake capacity of ZELDA increases with increasing oil-to-aqueous phase volume ratio, which is driven by the increase in the net pore volume. We demonstrate that the ZELDA can be cyclically reused via the simple regeneration procedure, and it can be magnetically functionalized for contactless maneuverability and removal. Further studies would be necessary to evaluate the biocompatibility and degradability of ZELDA in the environment. Our approach allows for overcoming the limitations of methods used previously for the synthesis of porous zein materials and provides a control over the surface wettability and magnetic responsiveness. This study lays a foundation for using zein-based

adsorbents for oil recovery applications, where the oil-laden porous material can be either regenerated or used directly as a fuel source.

5. Declaration of interests

The authors declare that they have no known competing financial interests or personal relationships that could have appeared to influence the work reported in this paper.

6. Funding

JGL was supported through Louisiana State University under the Economic Development Assistantship program. BB and KTV acknowledge the financial support from National Science Foundation (MPS-2032497).

7. Authors' contribution

BB and KTV conceived the project and designed the experiments. NPH performed the experiments, and NPH and JGL analysed the data following the directions from BB and KTV. All authors participated in writing the manuscript.

References

[1] Y. Cheng, X. Li, Q. Xu, O. Garcia-Pineda, O.B. Andersen, W.G. Pichel, SAR observation and model tracking of an oil spill event in coastal waters, Mar. Pollut. Bull. 62 (2011) 350–363. https://doi.org/10.1016/j.marpolbul.2010.10.005.

[2] D. Gupta, B. Sarker, K. Thadikaran, V. John, C. Maldarelli, G. John, Sacrificial amphiphiles: Eco-friendly chemical herders as oil spill mitigation chemicals, Sci. Adv. 1 (2015) e1400265. https://doi.org/10.1126/sciadv.1400265.

[3] R. Pagnucco, M.L. Phillips, Comparative effectiveness of natural by-products and synthetic sorbents in oil spill booms, J. Environ. Manage. 225 (2018) 10–16. https://doi.org/10.1016/j.jenvman.2018.07.094.

[4] R.C. Prince, Oil Spill Dispersants: Boon or Bane?, Environ. Sci. Technol. 49 (2015) 6376–6384. https://doi.org/10.1021/acs.est.5b00961.

[5] C. Teas, S. Kalligeros, F. Zanikos, S. Stournas, E. Lois, G. Anastopoulos, Investigation of the effectiveness of absorbent materials in oil spills clean up, Desalination. 140 (2001) 259–264. https://doi.org/10.1016/S0011-9164(01)00375-7.

[6] M. Omarova, L.T. Swientoniewski, I.K. Mkam Tsengam, D.A. Blake, V. John, A. McCormick, G.D. Bothun, S.R. Raghavan, A. Bose, Biofilm Formation by Hydrocarbon-Degrading Marine Bacteria and Its Effects on Oil Dispersion, ACS Sustain. Chem. Eng. 7 (2019) 14490–14499. https://doi.org/10.1021/acssuschemeng.9b01923.

[7] J. Song, S. Rezaee, W. Guo, B. Hernandez, M. Puerto, F.M. Vargas, G.J. Hirasaki, S.L. Biswal, Evaluating physicochemical properties of crude oil as indicators of low-salinity–induced wettability alteration in carbonate minerals, Sci. Rep. 10 (2020) 1–16. https://doi.org/10.1038/s41598-020-60106-2.

[8] E. National Academies of Sciences, The Use of Dispersants in Marine Oil Spill Response, Washington, DC, 2019. https://doi.org/10.17226/25161.

[9] A.C. Bejarano, E. Levine, A.J. Mearns, Effectiveness and potential ecological effects of offshore surface dispersant use during the Deepwater Horizon oil spill: a retrospective analysis of monitoring data, Environ. Monit. Assess. 185 (2013) 10281–10295. https://doi.org/10.1007/s10661-013-3332-y.

[10] P. Somasundaran, P. Patra, R.S. Farinato, K. Papadopoulos, eds., Oil Spill Remediation, John Wiley & Sons, Inc, Hoboken, NJ, 2014. https://doi.org/10.1002/9781118825662.

[11] R.S. Judson, M.T. Martin, D.M. Reif, K.A. Houck, T.B. Knudsen, D.M. Rotroff, M. Xia, S. Sakamuru, R. Huang, P. Shinn, C.P. Austin, R.J. Kavlock, D.J. Dix, Analysis of Eight Oil

Spill Dispersants Using Rapid, In Vitro Tests for Endocrine and Other Biological Activity, Environ. Sci. Technol. 44 (2010) 5979–5985. https://doi.org/10.1021/es102150z.
[12] M.J. Hemmer, M.G. Barron, R.M. Greene, Comparative toxicity of eight oil dispersants, Louisiana sweet crude oil (LSC), and chemically dispersed LSC to two aquatic test species, Environ. Toxicol. Chem. 30 (2011) 2244–2252. https://doi.org/10.1002/etc.619.
[13] J. Sayyad Amin, M. Vared Abkenar, S. Zendehboudi, Natural Sorbent for Oil Spill Cleanup from Water Surface: Environmental Implication, Ind. Eng. Chem. Res. 54 (2015) 10615–10621. https://doi.org/10.1021/acs.iecr.5b01715.
[14] A. Bayat, S.F. Aghamiri, A. Moheb, G.R. Vakili-Nezhaad, Oil Spill Cleanup from Sea Water by Sorbent Materials, Chem. Eng. Technol. 28 (2005) 1525–1528. https://doi.org/10.1002/ceat.200407083.
[15] V.H. Pham, J.H. Dickerson, Superhydrophobic silanized melamine sponges as high efficiency oil absorbent materials, ACS Appl. Mater. Interfaces. 6 (2014) 14181–14188. https://doi.org/10.1021/am503503m.
[16] G. Wang, H. Uyama, Facile synthesis of flexible macroporous polypropylene sponges for separation of oil and water, Sci. Rep. 6 (2016) 21265. https://doi.org/10.1038/srep21265.
[17] M. Sun, W. Chen, X. Fan, C. Tian, L. Sun, H. Xie, Cooperative recyclable magnetic microsubmarines for oil and microplastics removal from water, Appl. Mater. Today. 20 (2020) 100682. https://doi.org/10.1016/j.apmt.2020.100682.
[18] K. Law, R.C. Thompson, Microplastics in the seas - Concern is rising about widespread contamination of the marine environment by microplastics, Science (80-.). 345 (2014) 144–145. https://doi.org/10.1002/2014EF000240/polymer.
[19] E. Huerta Lwanga, J. Mendoza Vega, V. Ku Quej, J. de los A. Chi, L. Sanchez del Cid, C. Chi, G. Escalona Segura, H. Gertsen, T. Salánki, M. van der Ploeg, A.A. Koelmans, V. Geissen, Field evidence for transfer of plastic debris along a terrestrial food chain, Sci. Rep. 7 (2017) 14071. https://doi.org/10.1038/s41598-017-14588-2.
[20] P. Anastas, N. Eghbali, Green Chemistry: Principles and Practice, Chem. Soc. Rev. 39 (2010) 301–312. https://doi.org/10.1039/b918763b.
[21] I. Paraman, B.P. Lamsal, Recovery and characterization of α-Zein from corn fermentation coproducts, J. Agric. Food Chem. 59 (2011) 3071–3077. https://doi.org/10.1021/jf104529c.
[22] J. Dong, Q. Sun, J.Y. Wang, Basic study of corn protein, zein, as a biomaterial in tissue engineering, surface morphology and biocompatibility, Biomaterials. 25 (2004) 4691–4697. https://doi.org/10.1016/j.biomaterials.2003.10.084.
[23] R. Shukla, M. Cheryan, Zein: The industrial protein from corn, Ind. Crops Prod. 13 (2001) 171–192. https://doi.org/10.1016/S0926-6690(00)00064-9.
[24] Z. Pedram Rad, J. Mokhtari, M. Abbasi, Fabrication and characterization of PCL/zein/gum arabic electrospun nanocomposite scaffold for skin tissue engineering, Mater. Sci. Eng. C. 93 (2018) 356–366. https://doi.org/10.1016/j.msec.2018.08.010.
[25] H. Lian, X. Liu, Z. Meng, Enhanced mechanical and osteogenic differentiation performance of hydroxyapatite/zein composite for bone tissue engineering, J. Mater. Sci. 54 (2019) 719–729. https://doi.org/10.1007/s10853-018-2796-0.
[26] L. Vogt, L. Liverani, J.A. Roether, A.R. Boccaccini, Electrospun zein fibers incorporating poly(glycerol sebacate) for soft tissue engineering, Nanomaterials. 8 (2018) 1–16. https://doi.org/10.3390/nano8030150.
[27] T. Zhang, R.A. Sanguramath, S. Israel, M.S. Silverstein, Emulsion Templating: Porous Polymers and beyond, Macromolecules. 52 (2019) 5445–5479. https://doi.org/10.1021/acs.macromol.8b02576.
[28] V.O. Ikem, A. Menner, A. Bismarck, High-porosity macroporous polymers sythesized from titania-particle- stabilized medium and high internal phase emulsions, Langmuir. 26 (2010) 8836–8841. https://doi.org/10.1021/la9046066.
[29] Y. Zhang, S. Guo, W. Wu, Z. Qin, X. Liu, CO 2 -Triggered Pickering Emulsion Based on

Silica Nanoparticles and Tertiary Amine with Long Hydrophobic Tails, Langmuir. 32 (2016) 11861–11867. https://doi.org/10.1021/acs.langmuir.6b03034.
[30] D. Pradilla, S. Simon, J. Sjöblom, J. Samaniuk, M. Skrzypiec, J. Vermant, Sorption and Interfacial Rheology Study of Model Asphaltene Compounds, Langmuir. 32 (2016) 2900–2911. https://doi.org/10.1021/acs.langmuir.6b00195.
[31] R. Wang, W. Li, R. Lu, J. Peng, X. Liu, K. Liu, H. Peng, A facile synthesis of cationic and super-hydrophobic polyHIPEs as precursors to carbon foam and adsorbents for removal of non-aqueous-phase dye, Colloids Surfaces A Physicochem. Eng. Asp. 605 (2020) 125334. https://doi.org/10.1016/j.colsurfa.2020.125334.
[32] J. Tang, P.J. Quinlan, K.C. Tam, Stimuli-responsive Pickering emulsions: recent advances and potential applications, Soft Matter. 11 (2015) 3512–3529. https://doi.org/10.1039/C5SM00247H.
[33] M.S. Silverstein, PolyHIPEs: Recent advances in emulsion-templated porous polymers, Prog. Polym. Sci. 39 (2014) 199–234. https://doi.org/10.1016/j.progpolymsci.2013.07.003.
[34] N. Briggs, A.K.Y. Raman, L. Barrett, C. Brown, B. Li, D. Leavitt, C.P. Aichele, S. Crossley, Stable pickering emulsions using multi-walled carbon nanotubes of varying wettability, Colloids Surfaces A Physicochem. Eng. Asp. 537 (2018) 227–235. https://doi.org/10.1016/j.colsurfa.2017.10.010.
[35] D. Wang, S. Tao, S.W. Yin, Y. Sun, Y. Li, Facile preparation of zein nanoparticles with tunable surface hydrophobicity and excellent colloidal stability, Colloids Surfaces A Physicochem. Eng. Asp. 591 (2020) 124554. https://doi.org/10.1016/j.colsurfa.2020.124554.
[36] J.C. Prata, J.P. da Costa, I. Lopes, A.C. Duarte, T. Rocha-Santos, Environmental exposure to microplastics: An overview on possible human health effects, Sci. Total Environ. 702 (2020) 134455. https://doi.org/10.1016/j.scitotenv.2019.134455.
[37] A. Gálvez-Vergara, B. Fresco-Cala, S. Cárdenas, Switchable Pickering emulsions stabilized by polystyrene-modified magnetic nanoparticles, Colloids Surfaces A Physicochem. Eng. Asp. 606 (2020) 125462. https://doi.org/10.1016/j.colsurfa.2020.125462.
[38] S. Lu, D. Yang, M. Wang, M. Yan, Y. Qian, D. Zheng, X. Qiu, Pickering emulsions synergistic-stabilized by amphoteric lignin and SiO2 nanoparticles: Stability and pH-responsive mechanism, Colloids Surfaces A Physicochem. Eng. Asp. 585 (2020) 124158. https://doi.org/10.1016/j.colsurfa.2019.124158.
[39] M. Ago, S. Huan, M. Borghei, J. Raula, E.I. Kauppinen, O.J. Rojas, High-Throughput Synthesis of Lignin Particles (∼30 nm to ∼2 μm) via Aerosol Flow Reactor: Size Fractionation and Utilization in Pickering Emulsions, ACS Appl. Mater. Interfaces. 8 (2016) 23302–23310. https://doi.org/10.1021/acsami.6b07900.
[40] X. Chen, Y. Chen, L. Zou, X. Zhang, Y. Dong, J. Tang, D.J. McClements, W. Liu, Plant-Based Nanoparticles Prepared from Proteins and Phospholipids Consisting of a Core–Multilayer-Shell Structure: Fabrication, Stability, and Foamability, J. Agric. Food Chem. 67 (2019) 6574–6584. https://doi.org/10.1021/acs.jafc.9b02028.
[41] Y. Feng, Y. Lee, Surface modification of zein colloidal particles with sodium caseinate to stabilize oil-in-water pickering emulsion, Food Hydrocoll. 56 (2016) 292–302. https://doi.org/10.1016/j.foodhyd.2015.12.030.
[42] N. Bizmark, X. Du, M.A. Ioannidis, High Internal Phase Pickering Emulsions as Templates for a Cellulosic Functional Porous Material, ACS Sustain. Chem. Eng. 8 (2020) 3664–3672. https://doi.org/10.1021/acssuschemeng.9b06577.
[43] P.K. Vemula, G. John, Crops: A Green Approach toward Self-Assembled Soft Materials - Accounts of Chemical Research (ACS Publications), Acc. Chem. Res. 41 (2008) 769–782. http://pubs.acs.org/doi/full/10.1021/ar7002682#.
[44] T. Zhang, Y. Zhao, M.S. Silverstein, Cellulose-based, highly porous polyurethanes

templated within non-aqueous high internal phase emulsions, Cellulose. 27 (2020) 4007–4018. https://doi.org/10.1007/s10570-020-03059-z.
[45] X.H. Chen, C.H. Tang, Transparent high internal phase emulsion gels stabilized solely by proteins, Colloids Surfaces A Physicochem. Eng. Asp. 608 (2021) 125596. https://doi.org/10.1016/j.colsurfa.2020.125596.
[46] Y.-C. Yin, S.-H. Wen, C.-H. Tang, S.-W. Yin, K.-K. Li, X.-Q. Yang, Preparation of water-soluble antimicrobial zein nanoparticles by a modified antisolvent approach and their characterization, J. Food Eng. 119 (2013) 343–352. https://doi.org/10.1016/j.jfoodeng.2013.05.038.
[47] C.T. Rueden, J. Schindelin, M.C. Hiner, B.E. DeZonia, A.E. Walter, E.T. Arena, K.W. Eliceiri, ImageJ2: ImageJ for the next generation of scientific image data, BMC Bioinformatics. 18 (2017) 1–26. https://doi.org/10.1186/s12859-017-1934-z.
[48] H. Turasan, E.A. Barber, M. Malm, J.L. Kokini, Mechanical and spectroscopic characterization of crosslinked zein films cast from solutions of acetic acid leading to a new mechanism for the crosslinking of oleic acid plasticized zein films, Food Res. Int. 108 (2018) 357–367. https://doi.org/10.1016/j.foodres.2018.03.063.
[49] F.A. Momany, D.J. Sessa, J.W. Lawton, G.W. Selling, S.A.H. Hamaker, J.L. Willett, Structural characterization of α-zein, J. Agric. Food Chem. 54 (2006) 543–547. https://doi.org/10.1021/jf058135h.
[50] W. Shi, M.J. Dumont, Review: Bio-based films from zein, keratin, pea, and rapeseed protein feedstocks, J. Mater. Sci. 49 (2014) 1915–1930. https://doi.org/10.1007/s10853-013-7933-1.
[51] Y. Zhang, Y. Yang, K. Tang, Physicochemical Characterization and Antioxidant Activity of Quercetin-Loaded Chitosan Nanoparticles Yuying, Polym. Polym. Compos. 21 (2007) 449–456. https://doi.org/10.1002/app.
[52] J.M. Kliegman, R.K. Barnes, Glyoxal Derivatives. V. Reaction of Alcohols with Glyoxal, J. Org. Chem. 38 (1973) 556–560. https://doi.org/10.1021/jo00943a031.
[53] Y. Wang, G.W. Padua, Tensile Properties of Extruded Zein Sheets and Extrusion Blown Films, Macromol. Mater. Eng. 288 (2003) 886–893. https://doi.org/10.1002/mame.200300069.
[54] R. Ravikrishna, R. Green, K.T. Valsaraj, Polyaphrons as templates for the sol-gel synthesis of macroporous silica, J. Sol-Gel Sci. Technol. 34 (2005) 111–122. https://doi.org/10.1007/s10971-005-1329-x.
[55] B.D. Cassie, Of porous surfaces, (1944) 546–551.
[56] C.D. Johnson, F. Worrall, Novel low density granular adsorbents - Properties of a composite matrix from zeolitisation of vermiculite, Chemosphere. 68 (2007) 1153–1162. https://doi.org/10.1016/j.chemosphere.2007.01.049.
[57] F.X.B. Santosa, G.W. Padua, Tensile properties and water absorption of zein sheets plasticized with oleic and linoleic acids, J. Agric. Food Chem. 47 (1999) 2070–2074. https://doi.org/10.1021/jf981154p.
[58] J. Yin, C. Xiang, P. Wang, Y. Yin, Y. Hou, Biocompatible nanoemulsions based on hemp oil and less surfactants for oral delivery of baicalein with enhanced bioavailability, Int. J. Nanomedicine. 12 (2017) 2923–2931. https://doi.org/10.2147/IJN.S131167.
[59] Q. Wang, G.W. Padua, Properties of zein films coated with drying oils, J. Agric. Food Chem. 53 (2005) 3444–3448. https://doi.org/10.1021/jf047994n.
[60] H. Schulz, Oxidation of fatty acids, in: New Compr. Biochem., Elsevier Masson SAS, 1996: pp. 75–99. https://doi.org/10.1016/S0167-7306(08)60510-4.
[61] C. Zhang, W. Zhou, Q. Wang, H. Wang, Y. Tang, K.S. Hui, Comparison of static contact angle of various metal foams and porous copper fiber sintered sheet, Appl. Surf. Sci. 276 (2013) 377–382. https://doi.org/10.1016/j.apsusc.2013.03.101.
[62] A.A. Nikkhah, H. Zilouei, A. Asadinezhad, A. Keshavarz, Removal of oil from water using

polyurethane foam modified with nanoclay, Chem. Eng. J. 262 (2015) 278–285. https://doi.org/10.1016/j.cej.2014.09.077.
[63] I. Langmuir, THE CONSTITUTION AND FUNDAMENTAL PROPERTIES OF SOLIDS AND LIQUIDS. II. LIQUIDS. 1, J. Am. Chem. Soc. 39 (1917) 1848–1906. https://doi.org/10.1021/ja02254a006.
[64] Y. Ma, Y. Wu, J.G. Lee, L. He, G. Rother, A.L. Fameau, W.A. Shelton, B. Bharti, Adsorption of Fatty Acid Molecules on Amine-Functionalized Silica Nanoparticles: Surface Organization and Foam Stability, Langmuir. 36 (2020) 3703–3712. https://doi.org/10.1021/acs.langmuir.0c00156.
[65] J. Wang, Y. Zheng, A. Wang, Superhydrophobic kapok fiber oil-absorbent: Preparation and high oil absorbency, Chem. Eng. J. 213 (2012) 1–7. https://doi.org/10.1016/j.cej.2012.09.116.
[66] M.I. Al-Biloushi, H. Milliman, M.D. Gawryla, D.A. Schiraldi, Oil absorption performance of polymer/clay aerogel materials, J. Appl. Polym. Sci. 135 (2018) 45844. https://doi.org/10.1002/app.45844.
[67] J. Ge, F. Wang, X. Yin, J. Yu, B. Ding, Polybenzoxazine-Functionalized Melamine Sponges with Enhanced Selective Capillarity for Efficient Oil Spill Cleanup, ACS Appl. Mater. Interfaces. 10 (2018) 40274–40285. https://doi.org/10.1021/acsami.8b14052.
[68] F. Ludwig, O. Kazakova, L.F. Barquín, A. Fornara, L. Trahms, U. Steinhoff, P. Svedlindh, E. Wetterskog, Q.A. Pankhurst, P. Southern, P. Morales, M.F. Hansen, C. Frandsen, E. Olsson, S. Gustafsson, N. Gehrke, K. Lüdtke-Buzug, C. Grüttner, C. Jonasson, C. Johansson, Magnetic, structural, and particle size analysis of single- and multi-core magnetic nanoparticles, IEEE Trans. Magn. 50 (2014) 4–7. https://doi.org/10.1109/TMAG.2014.2321456.
[69] Z. Sun, L. Wang, P. Liu, S. Wang, B. Sun, D. Jiang, F.S. Xiao, Magnetically motive porous sphere composite and its excellent properties for the removal of pollutants in water by adsorption and desorption cycles, Adv. Mater. 18 (2006) 1968–1971. https://doi.org/10.1002/adma.200600337.
[70] Q. Zhu, F. Tao, Q. Pan, Fast and selective removal of oils from water surface via highly hydrophobic core-shell Fe2O3@C nanoparticles under magnetic field, ACS Appl. Mater. Interfaces. 2 (2010) 3141–3146. https://doi.org/10.1021/am1006194.
[71] A. Pavía-Sanders, S. Zhang, J.A. Flores, J.E. Sanders, J.E. Raymond, K.L. Wooley, Robust magnetic/polymer hybrid nanoparticles designed for crude oil entrapment and recovery in aqueous environments, ACS Nano. 7 (2013) 7552–7561. https://doi.org/10.1021/nn401541e.
[72] C.T. Cloney, R.C. Ripley, M.J. Pegg, P.R. Amyotte, Laminar burning velocity and structure of coal dust flames using a unity Lewis number CFD model, Combust. Flame. 190 (2018) 87–102. https://doi.org/10.1016/j.combustflame.2017.11.010.
[73] P.L. Lizotte, P. Savoie, A. De Champlain, Ash content and calorific energy of corn stover components in eastern Canada, Energies. 8 (2015) 4827–4838. https://doi.org/10.3390/en8064827.